











## ORIGINAL ARTICLE

# Reduction of exposure to simulated respiratory aerosols using ventilation, physical distancing, and universal masking

Jayne P. Coyle  | Raymond C. Derk  | William G. Lindsley  | Theresa Boots  |  
Francoise M. Blachere  | Jeffrey S. Reynolds | Walter G. McKinney  |  
Erik W. Sinsel  | Angela R. Lemons  | Donald H. Beezhold  | John D. Noti 

Health Effects Laboratory Division,  
Centers for Disease Control and  
Prevention, National Institute for  
Occupational Safety and Health,  
Morgantown, West Virginia, USA

## Correspondence

William G. Lindsley, National Institute  
for Occupational Safety and Health  
(NIOSH), 1000 Frederick Lane, M/S 4020,  
Morgantown, WV 26508-5402, USA.  
Email: wlindsley@cdc.gov

## Funding information

This work was supported by the Centers  
for Disease Control and Prevention  
Emergency Operations Center.

## Abstract

To limit community spread of SARS-CoV-2, CDC recommends universal masking indoors, maintaining 1.8 m of physical distancing, adequate ventilation, and avoiding crowded indoor spaces. Several studies have examined the independent influence of each control strategy in mitigating transmission in isolation, yet controls are often implemented concomitantly within an indoor environment. To address the influence of physical distancing, universal masking, and ventilation on very fine respiratory droplets and aerosol particle exposure, a simulator that coughed and exhaled aerosols (the source) and a second breathing simulator (the recipient) were placed in an exposure chamber. When controlling for the other two mitigation strategies, universal masking with 3-ply cotton masks reduced exposure to 0.3–3  $\mu\text{m}$  coughed and exhaled aerosol particles by >77% compared to unmasked tests, whereas physical distancing (0.9 or 1.8 m) significantly changed exposure to cough but not exhaled aerosols. The effectiveness of ventilation depended upon the respiratory activity, that is, coughing or breathing, as well as the duration of exposure time. Our results demonstrate that a layered mitigation strategy approach of administrative and engineering controls can reduce personal inhalation exposure to potentially infectious very fine respiratory droplets and aerosol particles within an indoor environment.

## KEYWORDS

exposure reduction, physical distancing, universal masking, ventilation

## 1 | INTRODUCTION

The association between human respiratory infection transmission by respiratory droplets and aerosols is well-established for several known pathogens.<sup>1</sup> Given that the average individual spends >90% of their day indoors,<sup>2</sup> there has been intense focus on factors associated with indoor transmission of SARS-CoV-2, the virus that causes COVID-19.<sup>3–5</sup> Epidemiological investigations highlight the role of congested, poorly ventilated spaces with high levels of

secondary attack rates and community transmission.<sup>6,7</sup> While the specific contribution of respiratory droplets and aerosols remains a topic of active research, increasing evidence of asymptomatic and pre-symptomatic individuals<sup>8</sup> contributing to community COVID-19 transmission suggests that very fine respiratory droplets and aerosol particles, that is, submicron particles to a few microns in diameter, can spread SARS-CoV-2.<sup>9</sup> To minimize exposure risks, the Centers for Disease Control and Prevention (CDC) recommends several mitigation strategies to limit COVID-19 transmission, including wearing

This is an open access article under the terms of the Creative Commons Attribution License, which permits use, distribution and reproduction in any medium, provided the original work is properly cited.

Published 2022. This article is a U.S. Government work and is in the public domain in the USA. Indoor Air published by John Wiley & Sons Ltd.

masks, maintaining physical distances, and avoiding crowded indoor and outdoor spaces, among other strategies.<sup>10,11</sup>

Universal masking reduces respiratory aerosol exposure through source control, that is, limiting the release of infectious very fine respiratory droplets and aerosol particles into the ambient environment at the point of generation, while face masks also provide some protection from aerosols for the mask wearer.<sup>12</sup> While the generalized effectiveness of masking for source control has been established,<sup>13–15</sup> its effectiveness is neither absolute nor uniform in practice. Variations in filtration efficiency, air flow resistance, user compliance, and mask fit can limit the effectiveness of masks as source control and protection for the wearer.<sup>16,17</sup> Despite these limitations, comparison of COVID-19 cases among states employing mask mandates demonstrate an association between universal masking and reduced incidence rates<sup>18–20</sup> as well as community transmission of COVID-19.<sup>21,22</sup>

Physical distancing reduces infectious material transfer via respiratory-derived droplets and aerosol particles. Routine respiratory actions, such as breathing and normal speech, produce micron and submicron scale particles that can remain airborne for minutes to hours.<sup>23</sup> By comparison, coughing, loud speech, and singing can project aerosols and droplets over greater distances, thus potentially increasing the probability for pathogen transmission. For example, droplets and aerosols produced by coughing may travel up to 8 m.<sup>24</sup> Analysis of a super spreader event among a cohort of choir members, all of whom were unmasked and within 1.8 m of physical distance during practice, estimated the SARS-CoV-2 attack rate as between 53.3% and 86.7%.<sup>25</sup> Correlative analyses support an association between physical distancing policies and reduction in COVID-19 incidence,<sup>26,27</sup> and agree with case-control studies.<sup>28</sup>

Engineering controls, such as room ventilation, are an effective and reliable strategy to ensure good air quality while mitigating infection transmission in the indoor environment.<sup>9,29</sup> While evidence clearly shows increasing ventilation rates as an effective measure in exposure mitigation,<sup>30,31</sup> air flow patterns can influence the dispersion of potentially infectious respiratory aerosols and personal exposure,<sup>32</sup> particularly in confined spaces.<sup>33</sup> The overall effectiveness of ventilation can be difficult to generalize since ventilation is unique to each room and operates alongside other exposure mitigating strategies, such as masking and physical distancing. As such, the current investigation examines the combined effect of physical distancing, universal masking, and ventilation on exposure to simulated very fine respiratory droplets and aerosol particles generated during breathing and coughing within a controlled indoor environment. The results of this investigation quantitatively examine the contribution of the matrix of controls employed on respiratory infection mitigation strategies within the indoor environment.

## 2 | MATERIALS AND METHODS

### 2.1 | Environmental chamber and ventilation

The testing environment consisted of an environment chamber measuring 3.15 m × 3.15 m × 2.26 m (gross internal volume of 23.8 m<sup>3</sup>, Figure 1). An internal re-circulating high-efficiency particulate air (HEPA) filtration

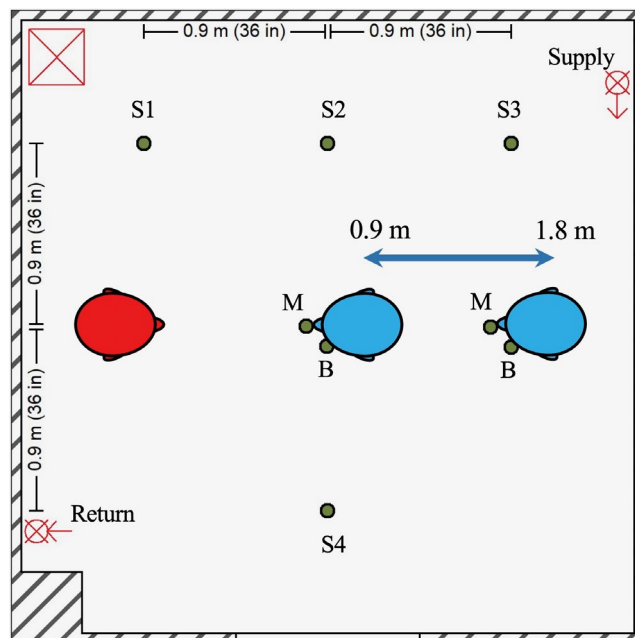


**FIGURE 1** Experimental setup and simulators. Diagram of environmental chamber setup showing positions of the aerosol source simulator (red), recipient simulators (blue; position adjustable between 0.9 and 1.8 m), and OPCs (green dots) for area measurements (S1–4) and personal breathing zone measurements at the mouth (M) and beside the head (B) of the recipient. The room air supply (at the ceiling) and return (near the floor) for the HEPA system are each shown with a circle and “X.” The HEPA filter and blower unit are demarcated by the red square containing an “X”

system (Flow Sciences, Inc.) was used to reduce background aerosol/particle concentrations to near-zero prior to each experiment. The HEPA system consisted of a 10.8 cm return duct positioned along the left wall 55.9 cm from the ground leading to the central motor/filter unit and a supply duct positioned along the right wall at a height of 2.19 m from the floor; no external fresh air was introduced into the environmental chamber during experimentation. The HEPA system utilized for experimentation was configured for dilution ventilation for our experiments in order to maximize the removal of aerosol particles from the test chamber. Six Grimm 1.108 optical particle counters (OPCs; GRIMM Aerosol Technik Ainring GmbH & Co. KG) were positioned at a height of 152 cm throughout the chamber. The OPCs measured particle concentrations in channels ranging from 0.3 to 3.0  $\mu\text{m}$  at a frequency of 1 Hz, except for one OPC sampler at 0.167 Hz. Four OPCs were affixed to telescopic stands 152 cm above the floor and referred to as “area samplers.” One OPC was positioned 3.2 cm next to the mouth central axis and anteriorly planar to the mouth opening of the recipient simulator (see below) and fit behind a mask affixed to the simulator; this position is denoted as “at the mouth of the breather” for presentation purposes. The remaining OPC was positioned 8.9 cm next to the mouth central axis and anteriorly planar to the mouth opening of the recipient simulator to allow for measurement in the personal breathing zone outside of a mask affixed to the simulator. All OPCs were controlled and data logged using a custom program in LabVIEW v. 2009 (National Instruments).

In addition to particle removal, the HEPA system provided ventilation, with a variable transformer (Staco Energy Products, Co.) used

to set the HEPA system flow rate. Air exchange rates were determined via single-point measurement of the linear air flow at the return duct using a Model 5725 VelociCalc rotating vane anemometer (TSI, Inc.) equipped with a tapered air cone (TSI, Inc.). The return duct was straightened for a length of >10 diameters from the return opening to minimize turbulent flow during anemometer readings for air changes per hour (ACH) derivation. The HEPA system was set to 0 ACH, 4 ACH (0.255 m<sup>3</sup>/s flow), 6 ACH (0.382 m<sup>3</sup>/s), and 12 ACH (0.765 m<sup>3</sup>/s); calculations assumed zero leakage into the chamber. Effective air filtration rates were derived empirically. Briefly, the chamber was saturated with particles using a stand-alone TSI Model 8026 generator until the 0.3–0.4 μm particle size channel reached 10<sup>5</sup> particles per liter under constant mixing using a household fan. The particles for effective air changes per hour were generated using a 1% solution of NaCl in distilled water formulated from 100 mg tablets provided with the TSI Model 8026 generator as per manufacturer's instructions. After a 15-min mixing period, the HEPA filtration system was set to the desired ACH based on anemometer measurements. Particle concentrations were measured for 20 min using five of the six OPCs to derive particle exponential decay curves spatially throughout the chamber. Theoretical particle exponential decay curves were modeled from the three smallest size bins (0.3–0.4 μm, 0.4–0.5 μm, and 0.5–0.65 μm) assuming negligible loss to chamber surfaces and aerosol agglomeration using MATLAB v. 9.6 (Mathworks). The slope of the modeled particle decay was assumed to be first order as per equation:

$$C_t = C_i e^{-\lambda t} \quad (1)$$

Where:

$C_t$  is the particle concentration at time  $t$  (#/cm<sup>3</sup>).

$C_i$  is the initial particle concentration at time zero (#/cm<sup>3</sup>).

$e$  is Euler's number, approximated to 2.71828.

$\lambda$  is the slope of particle concentration change over the time (#/cm<sup>3</sup>/s).

$t$  is time (s).

Empirical concentrations of particles measured by the five area OPCs were then fitted via log-linear regression and the resultant decay coefficient ( $\lambda$ ) derived to estimate the effective OPC-specific ACH.

## 2.2 | Aerosol source and simulators

The source simulator had a head form with pliable skin (Hanson Robotics) as described in previous work.<sup>14</sup> For these tests, a single cough and two versions of simulated breathing were examined. The simulated very fine respiratory droplets and aerosol particles (herein designated as aerosol) were produced with a 14% w/v KCl solution nebulized by a single jet Collision atomizer (BGI, Inc.) with an inlet pressure of 103 kPa (15 lbs./in<sup>2</sup>) prior to passive drying (Model 3062; TSI, Inc.), dilution with dry filtered air at 10 L/min (single cough tests) or 15 L/min (breathing tests), and neutralization by an ionizer (Model HPX-1, Electrostatics, Inc.). The coughing modality was performed by loading the simulator elastomeric bellows with test aerosol,

followed by a single 4.2 L rapid exhalation at a peak flow rate of 11 L/min<sup>33</sup>; the simulator did not breathe following the cough. For breathing tests, the simulator breathing rate was 12 breaths/min with a tidal volume of 1.25 L and ventilation rate of 15 L/min. The breathing parameters correspond to the ISO standard for females performing light work.<sup>34</sup> For the breathing modality, the nebulizer was cycled 10 s on and 50 s off continuously throughout the test duration. Tests were conducted for a duration of 15 min, except for a limited subset of testing conditions which were conducted for 60 min. As an additional examination of the time dependency of ventilation in reducing recipient exposure, additional tests were conducted using a modified aerosol generation cadence during the breathing action. During these tests, the nebulizer generated aerosol continuously for the first 3 min of the test, after which the nebulizer was turned off, and are henceforth designated short-term aerosol generation tests.

To simulate source aerosol exposure to a recipient, a breathing simulator (Warwick Technologies Ltd.) with a pliable skin head form (Respirator Testing Head Form 1–Static; Crawley Creatures Ltd.) was placed upon a mobile cart to enable alteration of the distance between source and the recipient. The mouth of the recipient simulator head form was positioned 152 cm above the floor. The simulator breathed with a sinusoidal waveform at 21.5 breaths/min with a ventilation rate of 27 L/min. These parameters are approximately the average of the ISO standards for males and females performing moderate work.<sup>34</sup> Both simulators were controlled during all experiments using custom scripted programs in LabVIEW.

## 2.3 | Experimental procedure

For experimental trials with masking conditions, a 3-ply cotton mask (Hanes Defender, HanesBrand, Inc.) was fitted to the respective simulator followed by fit factor assessment using the PortaCount Pro+ (TSI, Inc.) in the N95 mode (measuring negatively charged particles 55 nm in diameter)<sup>15</sup> as per manufacturer's instructions. A daily quality assurance test was conducted using the 3M 1860 N95 respirator (Saint Paul, MN).

To test the effect of layering aerosol mitigation strategies of universal masking, physical distancing, and ventilation, experiments consisting of a matrix of the three variables were conducted (Table 1). For masking, the combinations of no masking (neither simulator wore a mask) and universal masking (both simulators wore a 3-ply cotton mask) were examined. For physical distancing, given the limitation of the distance due to the size of the environmental chamber, 0.9 and 1.8 m distances were examined. For ventilation, four ACH rates were selected: 0, 4, 6, and 12.

After mask fitting and distance configuration, the environmental chamber was sealed, and the HEPA filtration system run at maximal rate to minimize background airborne particles. Thereafter, the HEPA filtration system was either turned off (0 ACH) or set to the desired air exchange rate (4–12 ACH) and allowed to run for 15 min, during which time all OPCs were initialized to begin particle concentration data collection and the recipient simulator activated to begin

breathing. After the air exchange stabilized, the source simulator was initiated to cough or breathe, and aerosol concentrations were measured for 15 min. The chamber was allowed to cool to 22°C between experiments to reduce the inter-test temperature variability. Three independent experimental replicates were conducted for each unique experimental condition without condition randomization.

## 2.4 | Data processing and statistical analysis

The background aerosol concentration was determined based on the mean particle concentration during the 3 min prior to cough or exhalation. The bin-specific particle counts per cubic meter of air were converted to volume based on the mean bin diameter (assuming spherical particles) and then to mass concentration by multiplying by the density of KCl (1.984 g/cm<sup>3</sup>). The total mass concentration was calculated by summing the bin-specific mass concentrations for all size bins. The mean mass concentration was calculated as the average mass concentration over the test duration and served as the exposure metric in these simulations. OPC data were processed using the R statistical environment v. 4.0.2 (R Project for Statistical Computing). All point estimates are presented as the arithmetic mean  $\pm$  1 standard deviation of the measured mean mass concentration.

Regression modeling was performed in R using the base linear model (*lm*) function using a logarithmic transformation of the mean mass concentration at the mouth of the breathing recipient against three predictor variables: Masking (Unmasked = 0 and Masked = 1; categorical); Distance (0.9 m = 0 and 1.8 m = 1; categorical); and Theoretical ACH (0, 4, 6, and 12; continuous). Comparisons of model fit with and without interaction between ACH and distance were conducted via an analysis of variance (ANOVA) test. Unstandardized regression coefficients are presented in addition to back-transformed coefficients expressed as percent reduction in the outcome variable (mean mass concentration). Statistical significance was set at  $p < 0.05$ .

## 3 | RESULTS AND DISCUSSION

### 3.1 | Chamber conditions, ventilation, and aerosol characterization

Across all experiments, the mean chamber temperature was  $24.1 \pm 1.1^\circ\text{C}$  with a relative humidity of  $26.0\% \pm 2.4\%$ . The temperature change during all experiments rose  $0.4^\circ\text{C} \pm 0.2^\circ\text{C}$  and the relative humidity change was  $0.2^\circ\text{C} \pm 0.2^\circ\text{C}$ . Particle clearance by the ventilation system followed first-order exponential decays, with overall clearance rates  $74.1\% \pm 4.4\%$  of decay rates estimated by anemometer readings (Range: 73.1%–76.7%; Figure 2A). Particle decay rates throughout the chamber, as measured by the five OPCs, were largely homogeneous (Figure S1). The experimental decay rates after single coughs were  $76.1\% \pm 1.5\%$  of theoretical values (Range: 74.4%–77.3%). These experimental decay rate magnitudes and variances were comparable to those obtained from particle decay testing, which suggests that the ventilation system promoted adequate air mixing to disperse cough aerosols through the chamber volume. Therefore, we presume similar air mixing within the chamber during ventilation studies for the other two modalities tested.

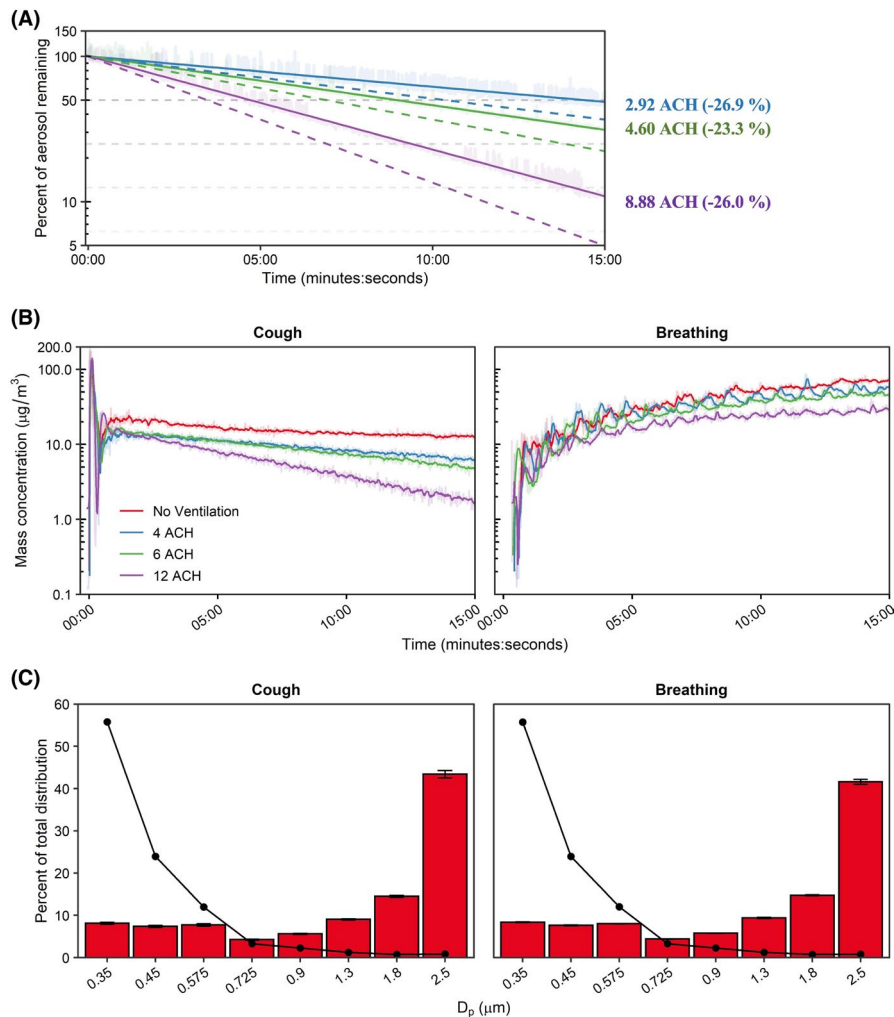
Chamber aerosol concentrations during simulated respiratory events are shown in Figure 2B. A single simulated cough produced an immediate aerosol influx within the chamber followed by mixing and log-linear decay, except for no ventilation in which the aerosol concentration reached a plateau. As expected, the continuous influx of aerosol during breathing resulted in an initial phase of rapid increase in aerosol particles which decelerated over time, suggesting a steady state between the source aerosol influx and removal by ventilation would be reached over longer testing durations. The bin-specific size and mass distributions of the KCl aerosol averaged over the test duration were similar across modalities. The particle size data indicated that 41.2%–44.4% of the aerosol mass was in the 2–3  $\mu\text{m}$  range (2.5  $\mu\text{m}$  channel) which tapered to a nadir between 4.1% and 4.4% among the 0.65–0.8  $\mu\text{m}$  size range (0.725  $\mu\text{m}$  channel). The remaining three

TABLE 1 Experimental parameters

Aerosol generation modality	Test duration (min)	Physical distance (m)	Ventilation rate (ACH)	Masking	Nebulizer and simulator
Cough	15	0.9 and 1.8	0, 4, 6, 12	No masks and universal masking	Nebulizer active during pre-cough inspiration and inactive for remainder of experiment
Breathing	15	0.9 and 1.8	0, 4, 6, 12	No masks and universal masking	Nebulizer active 10 s/inactive 50 s through duration of testing. Breathing continuous
Breathing	60	1.8	0, 4, 12	No masks and universal masking	Nebulizer active 10 s/inactive 50 s through duration of testing. Breathing continuous

Abbreviation: ACH, Air changes per hour.

**FIGURE 2** Ventilation and aerosol characterization. (A) Environmental chamber particle decay rates across HEPA ventilation settings. Dashed lines indicate the theoretical decay rate for each examined ventilation rate; solid lines indicate effective rates determined. Enumerated effective air exchange rates shown at the end time-point with percent error from theoretical (negative value indicates lower than theoretical). (B) Mean chamber mass concentration-time curves of simulated very fine respiratory droplets and aerosol particles for the examined respiratory actions and ventilation rates. (C) Bin-specific particle distributions as determined by mass (bars) and by number of particles (line). The median particle diameter ( $D_p$ ) indicates the bin. Results are the arithmetic mean  $\pm$  standard deviation of three independent experiments. Error bars for the number of particles (line) too small to visualize. ACH, Air changes per hour



smallest bins each registered between 7.1% and 8.4% of the mass distribution (Figure 2C). On a particle number basis, most particles were detected within the smallest size channel with <3% attributed to the largest size bin. Similar to the proportional mass distribution, particle count size distribution was analogous across the tested modalities and was similar the OPCs within the chamber (Figure S2). The proportional size distribution demonstrated a peak at  $0.35 \mu\text{m}$ —the smallest measured size bin—via OPC and was similar to tests measuring human respiratory aerosols via OPC-based measurements. Of note, the aerosol concentrations measured in the current investigation were 1–2 orders of magnitude higher than concentrations generated by typical human respiratory events.<sup>23,35–37</sup>

### 3.2 | Masking, physical distance, and ventilation

The time-concentration curves at the 1.8 m physical distance are shown in Figure 3A; analogous results for the 0.9 m physical distance are presented in Figure S3. For a single cough, aerosol concentrations decayed log-linearly after aerosol generation, while aerosol concentrations during breathing continually increased over time. Donning a 3-ply cotton mask blunted the height of the

time-concentration curves. The mean aerosol mass concentrations at the mouth of the breathing recipient over the testing duration are presented in Figure 3B. Overall, universal masking reduced particle exposure compared to unmasked conditions, while exposure reduction by distance and ventilation did not produce discernable patterns of exposure modulation. To determine the relative exposure reduction of universal masking, physical distancing, and ventilation during the 15-min tests, mean mass concentrations were regressed using ordinary least squares (OLS) multiple linear regression. Inclusion of the interaction term did not improve the model for either cough ( $p = 0.3062$ ) or breathing ( $p = 0.6475$ ) compared to models without interaction while also increasing the model Akaike's Information Criterion, thus, fixed effects OLS models without interaction were constructed. Results of multiple OLS regression are presented in Table 2. Interactions between masking and the other parameters were neither expected nor tested.

Adjusting for ACH and physical distance, universal masking significantly reduced aerosol exposure compared to unmasked exposures ( $p < 0.001$  among all modalities) during the 15-min tests. Fit factors of the 3-ply cloth mask were  $4.1 \pm 2.6$  ( $n = 43$ ) for the recipient and  $1.7 \pm 0.6$  ( $n = 42$ ) for the source simulator. The largest reduction in aerosol mass exposure was observed after a single cough

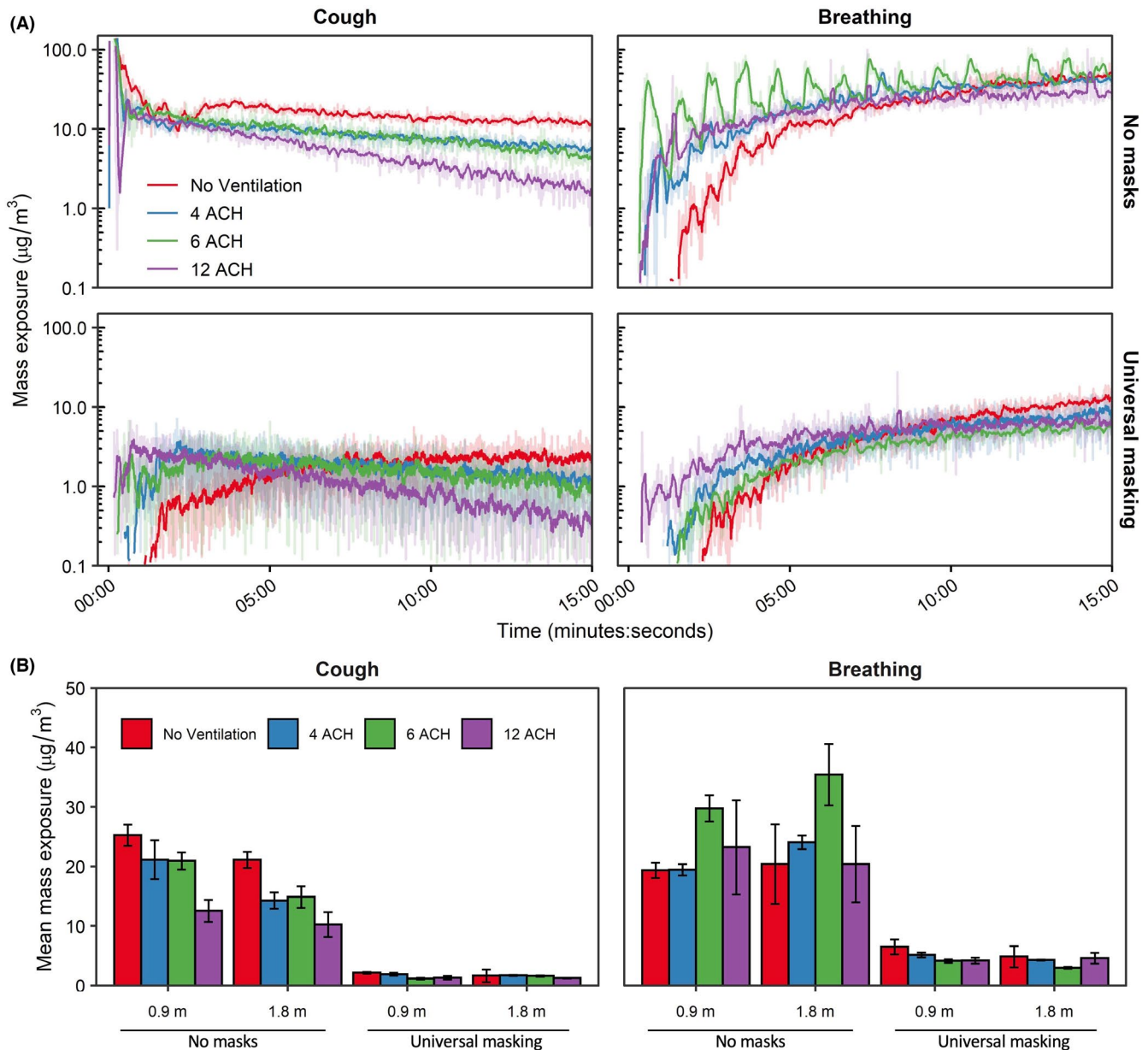


**FIGURE 3** Aerosol mass exposure of the recipient. (A) Mass exposure concentration over time across the matrix of modalities, masking status, and ventilation for the 1.8 m physical distance. Results for the 0.9 m physical distance are provided in the Figure S3. Data are the arithmetic mean of three independent experiments. (B) Mean mass exposure over the 15-min simulation period derived from the time curves. Results are the arithmetic mean  $\pm$  standard deviation of three independent experiments. No statistical comparisons were made between individual groups. ACH, Air changes per hour

(90.9%; 95% CI: 89.6%–91.9%), while exposure reduction was comparatively lower during breathing (80.8%; 95% CI: 77.5%–83.6%). The reduction in mass concentration was likely due to preferential filtration of aerosols  $>1 \mu\text{m}$  in diameter by the 3-ply cotton masks fitted to the source and recipient simulators (Figure 4). The differences in exposure reduction among the aerosol generation modalities were likely due to specific changes in aerosol spatiotemporal dispersion when the source was masked. Aerosol plumes generated during both breathing modalities and a single cough escape through face seal leaks.<sup>38</sup> The plumes would then be deflected behind and/or to the side of the source and thus effectively farther from the recipient

compared with the experiments with no masks. Without chamber mixing, as observed with no ventilation, the cough aerosol deflected by the mask took longer to disperse throughout the chamber compared to without a mask as was observed in Figure 3A. The time-concentration curves for breathing shifted to the right when masked, though not as much as after a single cough, showing that dispersion kinetics likely played a larger role in the heterogeneity observed for exposure reduction among the respiratory actions simulated here. While we cannot rule out the possibility that differential filtration of the source's mask was influenced by aerosol generation (for example, the higher expulsion velocity during coughing causing greater

TABLE 2 Regression coefficients for 15- and 60-min tests

Modality	Parameter	Regression coefficients		Percent reduction				Model adjusted R <sup>2</sup>
		$\beta$	95% CI	Estimate (%)	95% CI (%)	t-Value	Pr >  t	
Cough	Constant	3.146	3.010 to 3.282	–	–	46.587	<0.001	0.969
	Distance: 1.8 m	–0.167	–0.294 to –0.040	15.4	3.9 to 25.5	–2.656	0.011	
	ACH	–0.044	–0.059 to –0.030	4.3	2.9 to 5.7	–6.125	<0.001	
	Masking: Yes	–2.392	–2.519 to –2.265	90.9	89.6 to 91.9	–38.042	<0.001	
Breathing	Constant	3.203	3.034 to 3.373	–	–	38.129	<0.001	0.904
	Distance: 1.8 m	–0.060	–0.217 to 0.098	5.8	–10.3 to 19.5	–0.761	0.451	
	ACH	–0.006	–0.024 to 0.012	0.6	–1.2 to 2.4	–0.645	0.522	
	Masking: Yes	–1.650	–1.808 to –1.492	80.8	77.5 to 83.6	–21.091	<0.001	
Breathing 60 min <sup>a</sup>	Constant	4.569	4.438 to 4.699	–	–	74.588	<0.001	0.976
	ACH	–0.098	–0.112 to –0.083	9.0	7.7 to 10.3	–14.105	<0.001	
	Masking: Yes	–1.553	–1.700 to –1.406	76.0	72.8 to 78.8	–22.477	<0.001	

Abbreviation: ACH, Air changes per hour.

<sup>a</sup>Only the 0.9 m physical distancing configuration was examined.

mask aerosol filtration compared to breathing), our previous work suggests the aerosol generation modality likely does not influence mask collection efficiency for this 3-ply cotton mask ( $51.7\% \pm 7.1\%$  for coughing and  $44.3\% \pm 14.0\%$  for breathing).<sup>15</sup> Lastly, since the current investigation utilized static breathing simulators, the results do not account for the potential contribution of anthropogenic movement and individual behavior to aerosol particle exposure.<sup>39</sup> We have previously observed the presence of the exhalation from a breathing receiver can influence aerosol particle exposure within the experimental configuration contained in this work.<sup>12</sup> In a broader context, personal exposure within the indoor environment can be influenced by several factors, such as heterogeneous regions of aerosol concentration and changes in air flow patterns by individual bodily movements.<sup>40,41</sup> Therefore, while outside of the scope of the current investigation, anthropogenic factors should be considered especially when contextualizing the efficacy of examined exposure reduction mitigation strategies.

The exposure reductions associated with the other predictor variables varied depending on the respiratory action for the 15-min tests. When controlling for masking, increasing physical distance from 0.9 to 1.8 m significantly reduced aerosol exposure from a single cough by 15.4% (95% CI: 3.9%–25.5%;  $p = 0.011$ ); increasing ventilation also reduced exposure by 4.3% per ACH (95% CI: 2.9%–5.7%;  $p < 0.001$ ). Neither increasing ACH ( $p = 0.522$ ) nor increasing physical distance ( $p = 0.451$ ) provided protection during breathing for the 15-min tests. When extending the test duration to 60 min for breathing, the mean mass concentration from aerosol generation reached a dynamic equilibrium with each of the examined ACH rates (Figure 5). Analysis for the 60-min tests by OLS regression demonstrated increasing ventilation significantly decreased mean mass concentration by 9.0% (95% CI: 7.7%–10.3%;  $p < 0.001$ ; Table 2), while universal masking expectedly reduced mean mass concentration significantly.

When condensing the total aerosol generation period to the initial 3 min in the short-term aerosol generation tests, increasing ACH became a significant predictor in exposure reduction (5.2%; 95% CI: 3.8%–6.5%;  $p < 0.001$ ; Table S2). The time-concentration curves of the short-term aerosol generation tests demonstrated the log-linear decay similarly to time-concentration profiles observed from a single cough, albeit shifted to the right to reflect the longer aerosol generation period (Figure S4). This result demonstrates that attainment of a dynamic equilibrium with continuous aerosol input or removal of aerosols produced by an intense, short-term generation event through increasing ventilation can result in significant exposure reduction for a recipient. We did not examine the extended exposure duration for a single cough over 60 min, though we expect increasing ventilation will remain a significant predictor of mean mass concentration reduction.

With respect to ventilation, the restricted 15-min exposure duration contributed to the lack of pronounced effect of increasing ACH for breathing and can be explained when considering air flow. Ventilation not only provides contaminant removal but also impacts the overall air flow. Modeling of aerosol dispersion through central ventilation systems demonstrates this complex interplay between ventilatory clearance and overall air flow patterns that can, under certain situations, increase the short-term exposure during rapid, thorough mixing<sup>42</sup> that was observed during the breathing respiratory action. Increasing ventilation reduced monotonically the bulk aerosol concentration throughout the entire chamber over the total duration of the ventilation testing (Figure 3A) but tended to decrease the time of aerosol contact at the mouth of the recipient. Using a hand-held fog machine, smoke released at the position of the source's mouth tended to disperse initially, albeit slowly, in the direction of OPCs 2 and 3 (S2 and S3 as designated in Figure 1, respectively) under no ventilation and 4 ACH. With increasing ventilation,

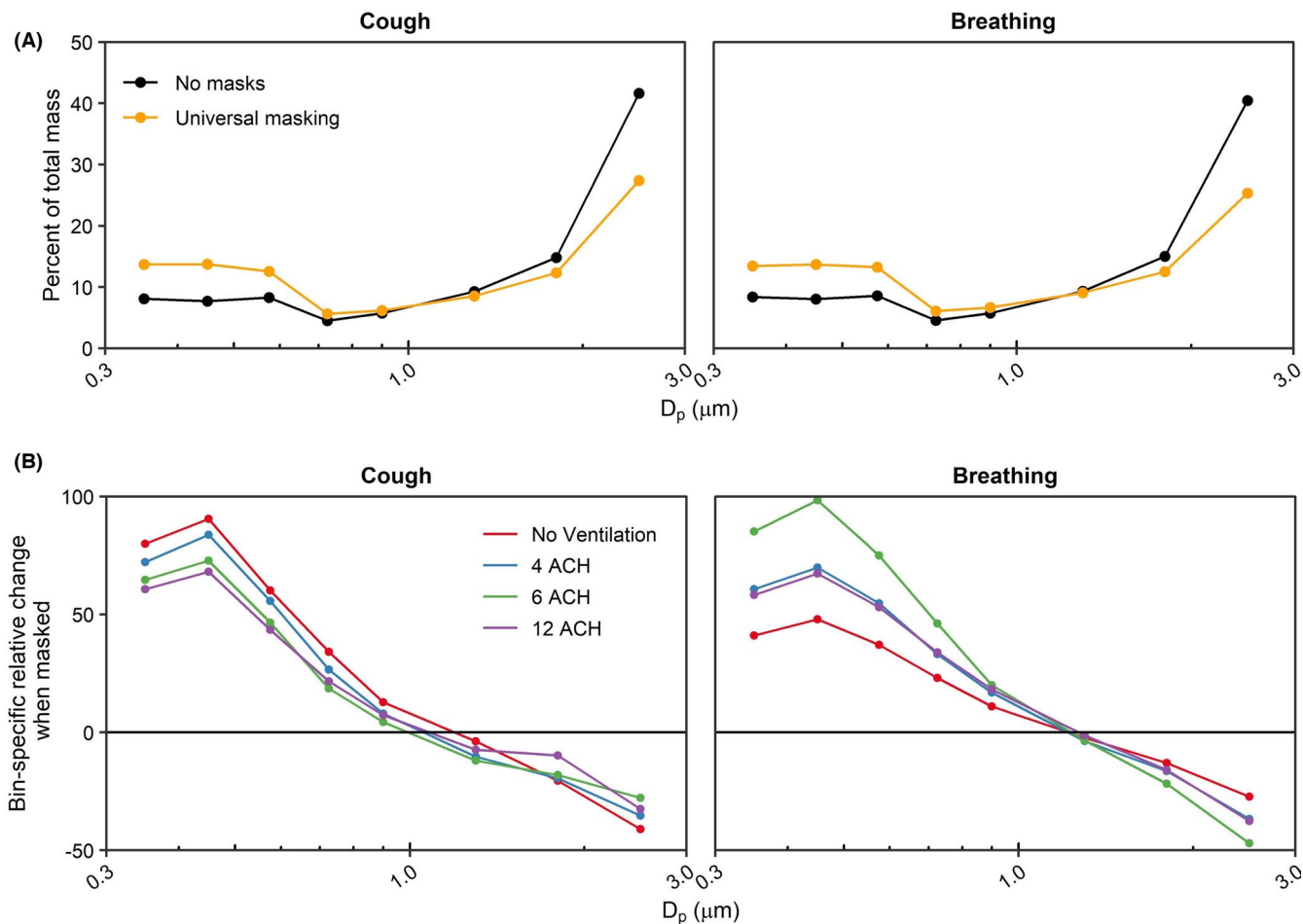


**FIGURE 4** Aerosol size distribution shifts during masking. (A) Bin-specific percent of mass distribution averaged across all ventilation rates. (B) Bin-specific percent change of aerosol distribution stratified by ventilation rate. The median particle diameter ( $D_p$ ) indicates the bin. Data are the arithmetic mean of three independent experiments. ACH, Air changes per hour

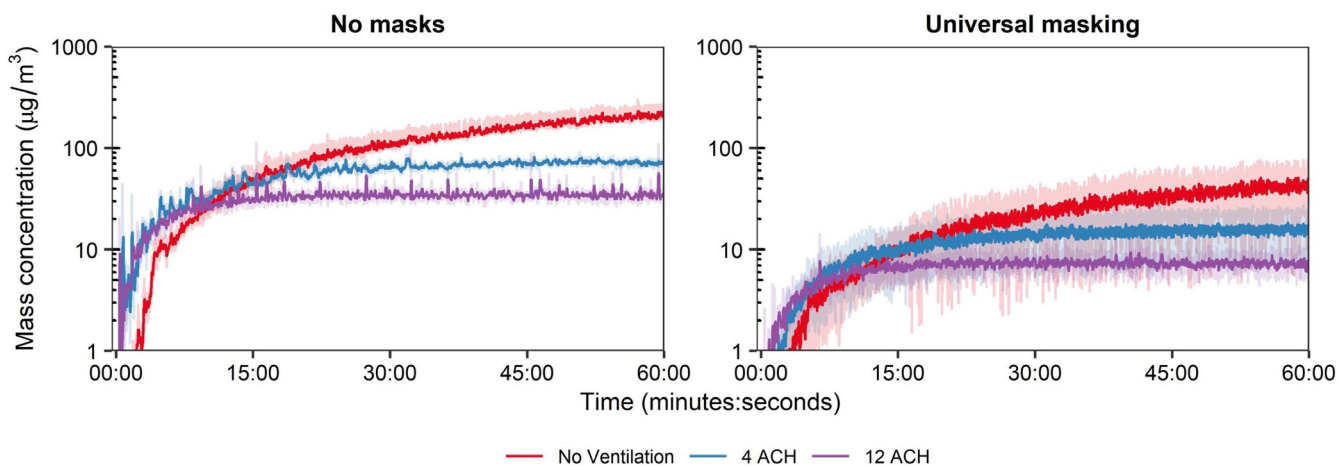


**FIGURE 5** Extended breathing assessment. Mass exposure concentration-time curves over 60 min for breathing at the 1.8 m physical distance and three ventilation rates. Results are the arithmetic mean  $\pm$  standard deviation of three independent experiments. ACH, Air changes per hour

the direction of initial smoke dispersion shifted toward the recipient, likely due to the pressure drop produced from the ventilation system supply stream above and behind the recipient (Figure S5). The

supply from 4 ACH traveled along the wall with the supply vent and deflected along the front wall prior to dissipation without a discernable air flow pattern. Increasing ventilation to 6 ACH lengthened the



travel distance along the front wall to include deflection along the intake wall as well as downwards toward the floor and in the direction of the Back Wall. Under 12 ACH, the air flow pattern followed that of 6 ACH, except the observed air flow along the Front Wall showed more diffuse downwards toward the floor and in the direction of the Back Wall; patterns along the Back Wall were not readily discernable at any ventilation tested. Examination of the OPC-stratified mean mass concentration-time series during breathing without masks and both respiratory actions during universal masking (Figures S6–S9) confirmed the qualitative air flow pattern suggested by the examination using the fog machine, suggesting air currents by the ventilation system in the environmental chamber was a significant contributor to dispersion during comparatively low-velocity aerosol particle release, such as during breathing and around face seal leaks for both respiratory actions. The initial high-velocity aerosol particles released during a cough without masking was comparatively unaffected by air currents described (Figure S8), while post-cough dispersion and mixing were influenced by air flow produced by the ventilation. Therefore, the air currents induced by the ventilation supply tended to influence recipient aerosol exposure where, in extreme cases, increasing ventilation paradoxically increased the receiver mean mass exposure (Figure 3B); this observation was largely independent of physical distance. Physical distance did contribute to aerosol dispersion with a physical distance of 0.9 m under no ventilation and without masking, where the exhalation from the receiver simulator likely increased the lateral dispersion aerosol particles from the source exhalation as reflected by the rapid increases in mean mass concentration measured by OPC sampler S4 (Figure S6) which was otherwise absent when positioned 1.8 m.

The authors opine such increases were caused by the observed thorough air mixing and changes in air flow patterning of aerosols after exhalation from the source, as was noted in particle decay studies and qualitative fog machine testing, in conjunction with the short exposure duration of 15 min. As previously noted, the effect of ventilation was appreciated during the 60-min breathing test and the short-term aerosol generation tests. These results demonstrate that the aerosol reduction measures by ventilation must consider the air mixing, aerosol spatial dispersion, and exposure duration in addition to other mitigation strategies to ascribe the degree of protection afforded. This becomes evident when examining the physical distancing within a well-mixed environment: the effectiveness of physical distancing can diminish.<sup>33,43,44</sup> Indeed, we observed apparent reduction in time to first contact with increasing ventilation at 0.9 m physical distancing (Figure S3) that was similar to the 1.8 m results. These results demonstrate that a complex interplay between air mixing and exposure duration can determine an individual's aerosol exposure.

### 3.3 | Limitations

The current investigation has several noteworthy limitations that must be considered. First, the mass concentration of

aerosol generated during the experimental modalities, particularly breathing, was higher than those produced from human exhalations.<sup>23</sup> The higher concentrations combined with the wide dynamic range of the OPC allowed for stable and reproducible measurements while assuring attainment of quantitative limits of detection among all tests. Second, the simulators lack generation of body heat, do not generate a thermal exhalation plume, and exhale or cough dry salt particles, all of which affect aerosol size, aerosol dispersion, and inhalation exposure.<sup>45–47</sup> Given the confines of the environmental chamber, the internal ventilation setup, and the high aerosol concentrations, we would not expect substantial differences in mean mass exposure given the small volume of the chamber. Therefore, limits must be placed on the interpretation of the results within a larger indoor environment, especially considering the dispersion potential of an exhalatory thermal plume and the strong influence of ventilation supply air flow observed. Third, the range of human respiratory aerosols can be smaller and larger than the measured range of this investigation (0.3–3.0  $\mu\text{m}$ ).<sup>35,37</sup> For droplets, the effect of physical distancing may be higher than those suggested by the observed results. Fourth, the study investigated the exposure reduction of a single 3-ply cotton mask. The authors recognize the limitation of having tested a single mask, since the effectiveness of exposure reduction by other masks could be either higher or lower, depending on the mask. Nonetheless, the analytics of the study allow for reasonable expectation of exposure reduction of the other predictor variables provided the aerosol behavior does not significantly deviate from this study with another type of mask.

## 4 | CONCLUSION

The current investigation highlights the contribution of three common engineering and administrative controls recommended for limiting SARS-CoV-2 exposure within an indoor environment: ventilation, physical distancing, and universal masking. When controlling for the other two mitigation strategies, universal masking with a 3-ply cotton mask contributed to the plurality of the observed reduction in aerosol mass exposure irrespective of aerosol generation modality. This reduction was due, in part, to preferential reduction of particles  $>1.0 \mu\text{m}$  in diameter from reaching the recipient. The overall effectiveness of ventilation and physical distancing was dependent upon the modality under simulated conditions. Although masking alone provided good exposure reduction, a layered mitigation approach<sup>48</sup> composed of engineering and administrative controls remains important in reducing an individual's personal exposure to potentially infectious very fine respiratory droplets and aerosol particles within an enclosed indoor space.

## ACKNOWLEDGMENTS

The authors wish to acknowledge the facilities, maintenance, and security personnel of NIOSH Morgantown for their hard work and dedication, which were integral to the completion of this work.

## CONFLICT OF INTEREST

The authors declare that they have no known competing financial interests or personal relationships that could have appeared to influence the work reported in this paper.

## AUTHOR CONTRIBUTIONS

Jayme P. Coyle involved in conceptualization, investigation, methodology, data curation, visualization, wrote the manuscript, and edited the manuscript. Raymond C. Derk involved in conceptualization, investigation, methodology, visualization, wrote the manuscript, and edited the manuscript. William G. Lindsley involved in conceptualization, investigation, methodology, software, wrote the manuscript, and edited the manuscript. Theresa Boots involved in formal analysis and edited the manuscript. Francoise M. Blachere involved in conceptualization, investigation, and edited the manuscript. Jeffrey S. Reynolds, Walter G. McKinney, and Erik W. Sinsel involved in methodology, software, and edited the manuscript. Angela R. Lemons involved in methodology, project administration, and edited the manuscript. Donald H. Beezhold and John D. Noti involved in project administration, supervision, funding acquisition, and edited the manuscript.

## DISCLAIMER

The findings and conclusions in this report are those of the authors and do not necessarily represent the official position of the National Institute for Occupational Safety and Health, Centers for Disease Control and Prevention. Mention of any company or product does not constitute endorsement by the National Institute for Occupational Safety and Health, Centers for Disease Control and Prevention.

## ORCID

Jayme P. Coyle  <https://orcid.org/0000-0002-4660-4710>

Raymond C. Derk  <https://orcid.org/0000-0003-3788-4551>

William G. Lindsley  <https://orcid.org/0000-0003-0720-5829>

Theresa Boots  <https://orcid.org/0000-0001-9469-3028>

Francoise M. Blachere  <https://orcid.org/0000-0003-1022-9741>

Walter G. McKinney  <https://orcid.org/0000-0002-5180-8451>

Erik W. Sinsel  <https://orcid.org/0000-0001-7929-7887>

Angela R. Lemons  <https://orcid.org/0000-0003-3057-9888>

Donald H. Beezhold  <https://orcid.org/0000-0001-5543-5747>

John D. Noti  <https://orcid.org/0000-0002-2927-9530>

## REFERENCES

- Jones RM, Brosseau LM. Aerosol transmission of infectious disease. *J Occup Environ Med*. 2015;57(5):501-508.
- Leech JA, Nelson WC, Burnett RT, Aaron S, Raizenne ME. It's about time: a comparison of Canadian and American time-activity patterns. *J Expo Anal Environ Epidemiol*. 2002;12(6):427-432.
- Qian H, Miao T, Liu L, Zheng X, Luo D, Li Y. Indoor transmission of SARS-CoV-2. *Indoor Air*. 2021;31(3):639-645.
- Nishiura H, Kobayashi T, Miyama T, et al. Estimation of the asymptomatic ratio of novel coronavirus infections (COVID-19). *Int J Infect Dis*. 2020;94:154-155.
- Shen J, Kong M, Dong B, Birnkrant MJ, Zhang J. Airborne transmission of SARS-CoV-2 in indoor environments: a comprehensive review. *Sci Technol Built Environ*. 2021;27(10):1331-1367.
- Lu J, Gu J, Li K, et al. COVID-19 outbreak associated with air conditioning in restaurant, Guangzhou, China, 2020. *Emerg Infect Dis*. 2020;26(7):1628-1631.
- Li Y, Qian H, Hang J, et al. Probable airborne transmission of SARS-CoV-2 in a poorly ventilated restaurant. *Build Environ*. 2021;196:107788.
- Furukawa NW, Brooks JT, Sobel J. Evidence supporting transmission of severe acute respiratory syndrome coronavirus 2 while pre-symptomatic or asymptomatic. *Emerg Infect Dis*. 2020;26(7):e1-e6.
- Morawska L, Allen J, Bahnfleth W, et al. A paradigm shift to combat indoor respiratory infection. *Science*. 2021;372(6543):689-691.
- CDC. CDC calls on Americans to wear masks to prevent COVID-19 spread. 2020. <https://www.CDC.gov/media/releases/2020/p0714-americans-to-wear-masks.html>. Accessed March 10, 2021
- CDC. Social Distancing: Keep a Safe Distance to Slow the Spread. 2020. <https://stacks.CDC.gov/view/cdc/90522>. Accessed March 10, 2021
- Lindsley WG, Beezhold DH, Coyle J, et al. Efficacy of universal masking for source control and personal protection from simulated cough and exhaled aerosols in a room. *J Occup Environ Hyg*. 2021;18(8):409-422.
- Leung NHL, Chu DKW, Shiu EYC, et al. Respiratory virus shedding in exhaled breath and efficacy of face masks. *Nat Med*. 2020;26(5):676-680.
- Lindsley WG, Blachere FM, Law BF, Beezhold DH, Noti JD. Efficacy of face masks, neck gaiters and face shields for reducing the expulsion of simulated cough-generated aerosols. *Aerosol Sci Technol*. 2021;55(4):449-457.
- Lindsley WG, Blachere FM, Beezhold DH, et al. A comparison of performance metrics for cloth face masks as source control devices for simulated cough and exhalation aerosols. *Aerosol Sci Technol*. 2021;55(10):1125-1142.
- Lawrence RB, Duling MG, Calvert CA, Coffey CC. Comparison of performance of three different types of respiratory protection devices. *J Occup Environ Hyg*. 2006;3(9):465-474.
- Oberg T, Brosseau LM. Surgical mask filter and fit performance. *Am J Infect Control*. 2008;36(4):276-282.
- Lyu W, Wehby GL. Community use of face masks and COVID-19: evidence from a natural experiment of state mandates in the US. *Health Aff (Millwood)*. 2020;39(8):1419-1425.
- Van Dyke ME, Rogers TM, Pevzner E, et al. Trends in county-level COVID-19 incidence in counties with and without a mask mandate - Kansas, June 1-August 23, 2020. *MMWR Morb Mortal Wkly Rep*. 2020;69(47):1777-1781.
- Guy GP Jr, Lee FC, Sunshine G, et al. Association of state-issued mask mandates and allowing on-premises restaurant dining with County-level COVID-19 case and death growth rates - United States, March 1-December 31, 2020. *MMWR Morb Mortal Wkly Rep*. 2021;70(10):350-354.
- Karaivanov A, Lu SE, Shigeoka H, Chen C, Pamplona S. Face masks, public policies and slowing the spread of COVID-19: evidence from Canada. *J Health Econ*. 2021;78:102475.
- Chernozhukov V, Kasahara H, Schrimpf P. Causal impact of masks, policies, behavior on early covid-19 pandemic in the U.S. *J Econom*. 2021;220(1):23-62.
- Asadi S, Wexler AS, Cappa CD, Barreda S, Bouvier NM, Ristenpart WD. Aerosol emission and superemission during human speech increase with voice loudness. *Sci Rep*. 2019;9(1):2348.
- Bourouiba L. Turbulent gas clouds and respiratory pathogen emissions: potential implications for reducing transmission of COVID-19. *JAMA*. 2020;323(18):1837-1838.

25. Hamner L, Dubbel P, Capron I, et al. High SARS-CoV-2 attack rate following exposure at a choir practice - Skagit county, Washington, March 2020. *MMWR Morb Mortal Wkly Rep.* 2020;69(19):606-610.
26. McGrail DJ, Dai J, McAndrews KM, Kalluri R. Enacting national social distancing policies corresponds with dramatic reduction in COVID-19 infection rates. *PLoS One.* 2020;15(7):e0236619.
27. Cobb JS, Seale MA. Examining the effect of social distancing on the compound growth rate of COVID-19 at the county level (United States) using statistical analyses and a random forest machine learning model. *Public Health.* 2020;185:27-29.
28. Fazio RH, Ruisch BC, Moore CA, Granados Samayoa JA, Boggs ST, Ladanyi JT. Social distancing decreases an individual's likelihood of contracting COVID-19. *Proc Natl Acad Sci USA.* 2021;118(8):e2023131118.
29. Luongo JC, Fennelly KP, Keen JA, Zhai ZJ, Jones BW, Miller SL. Role of mechanical ventilation in the airborne transmission of infectious agents in buildings. *Indoor Air.* 2016;26(5):666-678.
30. Sperna Weiland NH, Traversari R, Sinnige JS, et al. Influence of room ventilation settings on aerosol clearance and distribution. *Br J Anaesth.* 2021;126(1):e49-e52.
31. Somsen GA, van Rijn C, Kooij S, Bem RA, Bonn D. Small droplet aerosols in poorly ventilated spaces and SARS-CoV-2 transmission. *Lancet Respir Med.* 2020;8(7):658-659.
32. Noakes CJ, Sleight PA. Mathematical models for assessing the role of airflow on the risk of airborne infection in hospital wards. *J R Soc Interface.* 2009;6(Suppl 6):S791-800.
33. Lindsley WG, Blachere FM, McClelland TL, et al. Efficacy of an ambulance ventilation system in reducing EMS worker exposure to airborne particles from a patient cough aerosol simulator. *J Occup Environ Hyg.* 2019;16(12):804-816.
34. ISO. Respiratory protective devices - Human factors - Part 1: Metabolic rates and respiratory flow rates. ISO/TS 16976-1:2015. International Organization for Standardization, 2015.
35. Morawska L, Johnson GR, Ristovski ZD, et al. Size distribution and sites of origin of droplets expelled from the human respiratory tract during expiratory activities. *J Aerosol Sci.* 2009;40(3):256-269.
36. Johnson GR, Morawska L, Ristovski ZD, et al. Modality of human expired aerosol size distributions. *J Aerosol Sci.* 2011;42(12):839-851.
37. Holmgren H, Ljungstrom E, Almstrand A-C, Bake B, Olin A-C. Size distribution of exhaled particles in the range from 0.01 to 2.0µm. *J Aerosol Sci.* 2010;41(5):439-446.
38. Verma S, Dhanak M, Frankenfield J. Visualizing the effectiveness of face masks in obstructing respiratory jets. *Phys Fluids (1994).* 2020;32(6):061708.
39. Zhang N, Chen W, Chan PT, Yen HL, Tang JW, Li Y. Close contact behavior in indoor environment and transmission of respiratory infection. *Indoor Air.* 2020;30(4):645-661.
40. Han Z, To GN, Fu SC, Chao CY, Weng W, Huang Q. Effect of human movement on airborne disease transmission in an airplane cabin: study using numerical modeling and quantitative risk analysis. *BMC Infect Dis.* 2014;14:434.
41. Poussou SB, Mazumdar S, Plesniak MW, Sojka PE, Chen Q. Flow and contaminant transport in an airliner cabin induced by a moving body: model experiments and CFD predictions. *Atmos Environ.* 2010;44(24):2830-2839.
42. Pease LF, Wang N, Salsbury TI, et al. Investigation of potential aerosol transmission and infectivity of SARS-CoV-2 through central ventilation systems. *Build Environ.* 2021;197:107633.
43. Tang JW, Li Y, Eames I, Chan PK, Ridgway GL. Factors involved in the aerosol transmission of infection and control of ventilation in healthcare premises. *J Hosp Infect.* 2006;64(2):100-114.
44. Li Y, Leung GM, Tang JW, et al. Role of ventilation in airborne transmission of infectious agents in the built environment - a multidisciplinary systematic review. *Indoor Air.* 2007;17(1):2-18.
45. Sun S, Li J, Han J. How human thermal plume influences near-human transport of respiratory droplets and airborne particles: a review. *Environ Chem Lett.* 2021;19:1-12.
46. Vejerano EP, Marr LC. Physico-chemical characteristics of evaporating respiratory fluid droplets. *J R Soc Interface.* 2018;15(139):20170939.
47. Bourouiba L. Fluid dynamics of respiratory infectious diseases. *Annu Rev Biomed Eng.* 2021;23:547-577.
48. Shen J, Kong M, Dong B, Birnkrant MJ, Zhang J. A systematic approach to estimating the effectiveness of multi-scale IAQ strategies for reducing the risk of airborne infection of SARS-CoV-2. *Build Environ.* 2021;200:107926.

## SUPPORTING INFORMATION

Additional supporting information may be found in the online version of the article at the publisher's website.

**How to cite this article:** Coyle JP, Derk RC, Lindsley WG, et al. Reduction of exposure to simulated respiratory aerosols using ventilation, physical distancing, and universal masking. *Indoor Air.* 2022;32:e12987. doi:[10.1111/ina.12987](https://doi.org/10.1111/ina.12987)